Acta Crystallographica Section D
Biological Crystallography
ISSN 0907-4449

The structure and refinement of apocrustacyanin C_2 to 1.3 Å resolution and the search for differences between this protein and the homologous apoproteins A_1 and C_1

Jarjis Habash,[a] John R. Helliwell,[a]* James Raftery,[a] Michele Cianci,[b] Pierre J. Rizkallah,[b] Naomi E. Chayen,[c] Gwen A. Nneji[c] and Peter F. Zagalsky[d]

[a]Section of Structural Chemistry, Department of Chemistry, University of Manchester, Manchester M13 9PL, England, [b]Council for the Central Laboratory of the Research Councils, Daresbury Laboratory, Daresbury, Warrington WA4 4AD, England, [c]Biological Structure and Function Section, Division of Biomedical Sciences, Faculty of Medicine, Imperial College, London SW7 2AZ, England, and [d]Department of Molecular Biology and Biochemistry, Royal Holloway College, University of London, Egham, Surrey TW20 0EX, England

Correspondence e-mail: john.helliwell@man.ac.uk

Received 19 December 2003
Accepted 6 January 2004

PDB References: apocrustacyanin C_2 at 1.3 Å, 1s2p, r1s2psf; apocrustacyanin C_2 at 1.6 Å, 1s44, r1s44sf.

The blue carotenoprotein α-crustacyanin of *Homarus gammarus* lobster carapace is comprised chemically of five 20 kDa subunits. Only two genes for the proteins have been isolated (J. B. C. Findlay, personal communication) and the five apoproteins fall into two sets of homologous proteins based on their chemical properties (CRTC, consisting of apoproteins C_1, C_2 and A_1, and CRTA, consisting of apoproteins A_2 and A_3). The diffraction quality of apo C_2 has been improved from 2.2 to 1.3 Å and its structure solved. The structure is compared with the A_1 and C_1 proteins determined at 1.4 Å [Cianci *et al.* (2001), *Acta Cryst.* D**57**, 1219–1229] and 1.15 Å, respectively [Gordon *et al.* (2001), *Acta Cryst.* D**57**, 1230–1237] and found to be very similar. Normalized *B*-factor difference plots per residue of different types were used to try to find chemically modified residues; none were found at these resolutions. It remains possible that the differences between the CRTC proteins result from differences in amidation. By comparison of a crystal grown with glycerol (studied at 1.6 Å) and one grown without glycerol (studied at 1.3 Å) it was seen that glycerol bound at the astaxanthin site.

1. Introduction

α-Crustacyanin, the blue astaxanthin protein of lobster carapace, consists of two groups of homologous proteins (CRTC, containing apoproteins C_1, C_2 and A_1, and CRTA, containing apoproteins A_2 and A_3) based on their chromatographic properties and amino-acid sequence (Quarmby *et al.*, 1977; Findlay *et al.*, 1990; see Fig. 1). Recently substantial progress has been made in the study of the structures of crustacyanin. Cianci *et al.* (2001) reported the structure of apocrustacyanin A_1 using softer X-rays (2 Å wavelength) with a xenon derivative optimizing the $L_{\rm I}$ edge f'' (see also Olczak *et al.*, 2003) coupled with detecting the weak signal from S atoms *via* a high-redundancy data set protocol. This A_1 structure at 100 K was determined and refined to 1.4 Å resolution. Gordon *et al.* (2001) detailed the structure of the apocrustacyanin C_1 subunit of α-crustacyanin by phasing the crystal structure of a 40 kDa homodimer using the anomalous scattering from S atoms intrinsic to the native protein combined with direct methods. The C_1 structure (110 K) was refined to near-atomic 1.15 Å resolution. Cianci *et al.* (2002) used the A_1 as a molecular replacement model and thereby reported the molecular basis for the colouration mechanism in the lobster carapace of β-crustacyanin, a dimer of apoproteins A_1 and A_3 with two astaxanthin molecules, at 3.2 Å resolution. The study revealed the structural basis for the bathochromic shift of the astaxanthin spectrum in lobster β-crustacyanin. Astaxanthin (3,3′-dihydroxy-β,β′-carotene-4,4′-dione) dissolved in organic

Table 1
Data reduction showing completeness and mean $F/\sigma(F)$ for apocrustacyanin C_2 at 1.6 Å.

Values in parentheses represent the number of missing reflections. The overall merging R is 13.2%, crossing 35% at 1.79 Å. Allowing data inclusion with higher R factors (to 1.6 Å) is in agreement with the *CCP*4 Bulletin Board, which concluded in favour of $I/\sigma(I) > 1$ [*i.e.* $F/\sigma(F) > 2$], but we cut the data here at $I/\sigma(I) > 2$ [*i.e.* $F/\sigma(F) > 4$].

Resolution shells	Completeness (%)	Mean $F/\sigma(F)$	No. of reflections
∞–5.06	98.6	52.8	1714 (24)
5.06–3.58	99.9	54.9	2919 (2)
3.58–2.92	99.9	40.1	3696 (2)
2.92–2.53	99.8	24.4	4348 (7)
2.53–2.26	99.0	18.3	4862 (49)
2.26–2.07	98.8	14.9	5364 (66)
2.07–1.91	97.9	10.8	5816 (120)
1.91–1.79	97.6	6.7	6249 (151)
1.79–1.68	98.2	5.1	6611 (116)
1.68–1.60	97.7	4.1	6972 (158)

solvent is red/orange in colour (as in cooked lobster), but purple when protein-bound in β-crustacyanin. Zagalsky (2003) elaborated on the proposed mechanism of the bathochromic shift in protein-bound astaxanthin by comparison with several other related carotenoids and their spectra complexed with protein, noting that an explanation was lacking for the larger bathochromic shifts shown by some cyclopentenedione carotenoids in reconstituted carotenoproteins. Further work on these proteins involved a comparative study of the electron-density maps of apocrustacyanin C_1 produced from space- and earth-grown crystals (Habash *et al.*, 2003). The electron-density maps for the space-grown crystal were compared with those from the earth-grown crystal. Several of the residues with improved resolution for the space-grown crystal case were on the surface of the protein and two were at lattice contacts relevant to a possible improved crystal-growth mechanism in space. Most recently, we have reviewed progress to date including reporting the first ever diffracting crystals of α-crustacyanin (Chayen *et al.*, 2003). Here, we report the structure of apocrustacyanin C_2 refined to 1.3 Å resolution and the attempts made to find differences in the amino-acid side chains between the three homologous CRTC apoproteins C_1, C_2 and A_1.

2. Crystallization

α-Crustacyanin was extracted and purified from lobster carapace and apocrustacyanin C_2 was prepared as previously described for the A_2 subunit (Keen *et al.*, 1991), but using ethyl acetate/ether [3:1(*v*/*v*)] in place of acetone/ether to remove the carotenoid. The apoprotein (20 mg ml^{-1}) was prepared for crystallization in 0.1 *M* Tris–HCl, 1 m*M* EDTA pH 7 as described in Chayen *et al.* (1996). Crystals were grown in 2 µl drops by vapour diffusion in Linbro plates at 293 K. Crystallization conditions were based on the conditions described by Wright *et al.* (1992), who obtained crystals diffracting to 2.2 Å (using a stock of 20 mg ml^{-1} protein and a reservoir containing 0.1 *M* Tris–HCl pH 9.0, 1.4 *M* ammonium sulfate, 5% MPD and 1 m*M* EDTA). By reducing the protein concentration to 15 mg ml^{-1}, raising the ammonium sulfate concentration to 2.3 *M* and the addition of 20% glycerol, we obtained the crystals studied here to 1.6 Å. Crystals grown from 15 mg ml^{-1} protein solution over reservoirs containing 2.3 *M* ammonium sulfate, 5% MPD, 0.1 *M* Tris–HCl pH 7.0 and no glycerol appeared overnight, reached full size in 5 d and were studied here at 1.3 Å.

Table 2
Data reduction showing completeness and mean $F/\sigma(F)$ for apocrustacyanin C_2 at 1.3 Å.

Values in parentheses represent the number of missing reflections. The overall merging R is 8%, crossing 35% at 1.45 Å. See note in Table 1.

Resolution shells	Completeness (%)	Mean $F/\sigma(F)$	No. of reflections
∞–4.12	99.8	82.0	3109 (5)
4.12–2.90	100.0	84.3	5384 (0)
2.90–2.37	100.0	60.0	6849 (0)
2.37–2.05	99.8	39.8	8025 (16)
2.05–1.84	99.7	25.6	9072 (31)
1.84–1.68	99.9	13.4	9994 (13)
1.68–1.55	99.4	8.0	10823 (69)
1.55–1.45	97.6	5.5	11574 (277)
1.45–1.37	94.3	3.9	12322 (701)
1.37–1.30	89.3	3.6	13016 (1393)

3. Data collection and data reduction

Apocrustacyanin C_2 crystallizes in space group $P2_12_12_1$, with unit-cell parameters a = 41.15, b = 79.85, c = 110.26 Å for the 1.3 Å data set and a = 41.17, b = 79.88, c = 109.56 Å for the 1.6 Å data set. These are very similar to the published unit-cell data for apocrustacyanin A_1 and C_1. The two C_2 data sets were collected at the synchrotron-radiation beamline MPW14 (Duke *et al.*, 1998) at the SRS Daresbury Laboratory using single-crystal diffraction tuned to a wavelength of 0.9 Å; diffraction data were recorded on a CCD Quantum ADSC detector at cryotemperature. The exposure times were 20 s deg^{-1} for the 1.6 Å data set and 20 s 0.5 deg^{-1} (slow pass) and 10 s deg^{-1} (quick pass) for the 1.3 Å data set. The data were pocessed and merged using *MOSFLM* and *SCALA* (Leslie, 1992; Collaborative Computational Project, Number 4, 1994). Tables 1 and 2 summarize the data reduction and analyses of the two data sets.

4. Molecular structure

Apocrustacyanin C_2 crystallizes as a homodimer of 360 residues in the asymmetric unit. Each subunit has 180 amino-acid residues with a molecular weight of approximately 20 kDa, with an identical lipocalin structure to those reported for apocrustacyanin C_1 and A_1. The two subunits are related by a twofold non-crystallographic axis. N-terminal residue 1 is not visible in each subunit, as for apocrustacyanin A_1, in contrast to its analogue apocrustacyanin C_1, but is present in amino-acid sequence analysis of both C_2 and A_1 (as Asp) (Findlay *et al.*, 1990). Two differences in the sequence of apocrustacyanin A_1 from that of apocrustacyanin C_1 were suggested from crystal structure comparisons (Cianci *et al.*, 2001): Val at

residue 181, in place of Leu, and Asn at residue 5, in place of Asp. These replacements are re-examined here. The apocrustacyanin A_1 model of Cianci *et al.* (2001) was used for the apocrustacyanin C_2 refinement. A C^{α}-atom overlay of the molecular structures of apocrustacyanin A_1, C_1 and C_2 is shown in Fig. 2.

5. Structure refinement

Two data sets were used in this structure refinement. The first was the glycerol set to 1.6 Å resolution; these refined coordinates were then used (with glycerol and waters deleted) to refine the structure to 1.3 Å resolution against the second (non-glycerol) data set.

5.1. Structure refinement to 1.6 Å resolution (with glycerol)

The starting model was the deposited apocrustacyanin A_1 structure (PDB code 1h91; Cianci *et al.*, 2001). In the A_1 homodimer residue 1 is not visible; each chain has a peptide sequence consisting of residues 2–181. The bound waters were removed. After molecular replacement using *MOLREP* (Collaborative Computational Project, Number 4, 1994), the coordinates were subjected to a 0.25 Å perturbation in x, y and z as random shifts to remove any bias in the previous refinements. The model was first subjected to ten cycles of rigid-body refinement using *REFMAC*5 (Collaborative Computational Project, Number 4, 1994) with the R factor, $R_{\rm free}$ and FOM converging to 0.386, 0.375 and 0.609, respectively. Ten cycles of restrained with isotropic temperature-factor refinement then followed and the R factor, $R_{\rm free}$ and FOM converged to 0.281, 0.302 and 0.733, respectively. $2F_{\rm o} - F_{\rm c}$ and $F_{\rm o} - F_{\rm c}$ maps were generated using *FFT* (Collaborative Computational Project, Number 4, 1994) and were visualized using *O* (Jones *et al.*, 1991) on a Silicon Graphics computer system. Residue-by-residue inspection of the maps using 1 r.m.s. contour levels for $2F_{\rm o} - F_{\rm c}$ and 2 r.m.s. contour levels for $F_{\rm o} - F_{\rm c}$ showed that the model generally fitted the electron-density maps very well; only 12 side chains required refitting. The structure then underwent ten cycles of restrained isotropic temperature-factor refinement with the R factor, $R_{\rm free}$ and FOM converging to 0.229, 0.257 and 0.783,

Table 3
Final parameters for the refinement of the two data sets to 1.6 and 1.3 Å resolutions.

Values in parentheses are for the outer shell.

	1.6 Å	1.3 Å
Resolution range (Å)	64.55–1.6	64.55–1.3
Completeness (%)	98.6	97.2
No. reflections in working set	45426	81372
Free R value test-set size (%)	5.1	5.0
Free R value test-set count	2430	4296
No. non-H atoms used in refinement	3413	3411
R factor	0.203 (0.266)	0.189 (0.370)
$R_{\rm free}$	0.247 (0.324)	0.215 (0.425)
Mean B value (Å^2)	10.4	13.4
Mean B value (bound waters) (Å^2)	21.8	26.8
R.m.s. bond lengths, refined atoms (Å)	0.026	0.011
R.m.s. bond angles, refined atoms (°)	2.3	1.6
R.m.s. torsion angles (°)	5.8	5.2
Ramachandran plot statistics† (%)		
Residues in most favoured regions	91.2‡	91.6
Residues in additional allowed regions	8.1	7.8
Residues in generously allowed regions	0.0	0.0
Residues in disallowed regions§	0.6	0.6

† Calculated *via PROCHECK*; the other values were determined using *REFMAC*5 (both from the *CCP*4 program suite; Collaborative Computational Project, Number 4, 1994). § These are residues Tyr112*A* and Tyr112*B*; as noted previously in the structure analyses of Cianci *et al.* (2001) and Habash *et al.* (2003), they have strained conformations. ‡ 95% when the ice-ring-removed reflections are allowed for.

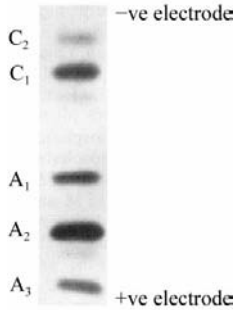

Figure 1
Dissociation of α-crustacyanin with 6 *M* urea and separation of the apoprotein subunits by 6 *M* urea–PAGE chromatography, showing the distinctive signatures of C_2, C_1, A_1, A_2 and A_3. Reprinted from Zagalsky & Tidmarsh (1985), copyright (1985), with permission from Elsevier.

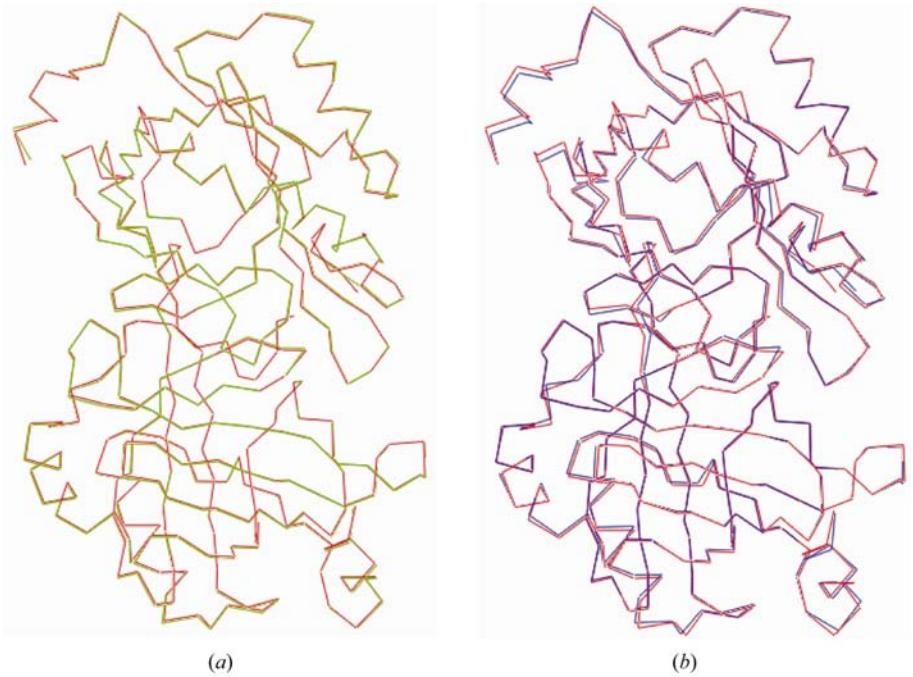

Figure 2
C^{α}-atom overlay of the molecular structures of apocrustacyanin. (*a*) C_2 (1.3 Å) in red and A_1 in green (r.m.s. *xyz* displacement 0.186 Å). (*b*) C_2 (1.3 Å) in red and C_1 in blue (r.m.s. *xyz* displacement 0.468 Å). The r.m.s. *xyz* displacement of the C^{α} atoms between the C_2 1.6 Å study and the C_2 1.3 Å study is 0.143 Å.

respectively. At this stage, *PEAKMAX* and *WATPEAK* (Collaborative Computational Project, Number 4, 1994) were used to generate the bound water structure and 220 water molecules were found. The structure with the protein and water molecules was subjected to three more iterations of refinement (each consisting of ten cycles); each iteration included inspecting the protein, adding new waters and deleting waters that failed to show reasonable (1 r.m.s.) $2F_o - F_c$ electron density or acceptable hydrogen bonds. The final R factor, R_{free} and FOM converged to 0.203, 0.247 and 0.793, respectively (see Table 3). This final model contained two sulfate ions, two MPDs, one glycerol and 479 water molecules. As a check of the agreement between this and the 1.6 Å bound solvent structure 367 bound water O atoms were within 1 Å of each other. Fig. 3 shows the glycerol electron-density maps and superimposed model.

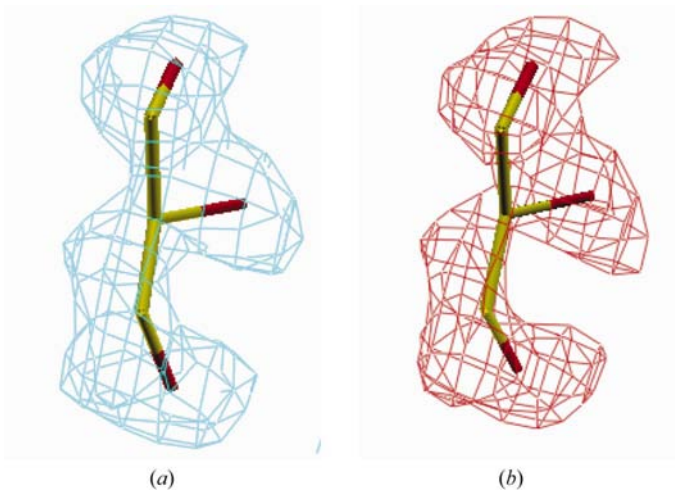

Figure 3
Section of protein electron-density map of apocrustacyanin C_2 from the 1.6 Å resolution data set, showing the glycerol molecule. (*a*) $2F_o - F_c$ at 1.0 r.m.s. contour level. (*b*) Omit map at 2.2 r.m.s. contour level.

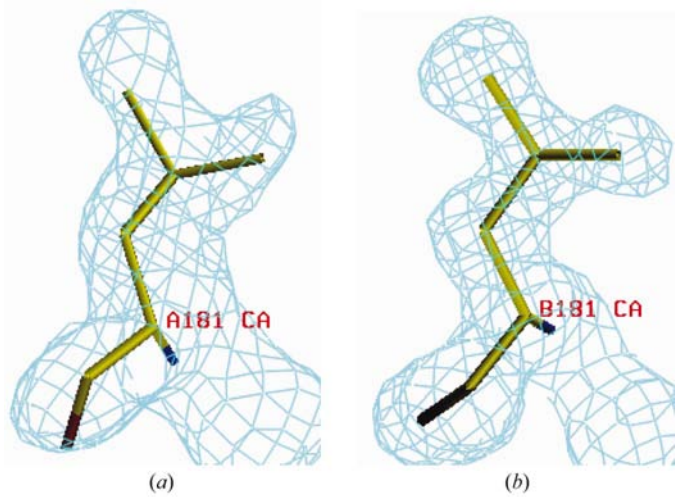

Figure 4
Section of $2F_o - F_c$ protein electron-density map at 1.0 r.m.s. contour level for apocrustacyanin C_2 to 1.3 Å resolution. (*a*) Leu181*A*, (*b*) Leu181*B*.

5.2. Structure refinement of the data set to 1.3 Å resolution (without glycerol)

The final model from §5.1 was used as the starting model for this refinement to 1.3 Å resolution. After removing the water molecules and the glycerol, essentially the same protocol was applied. After ten cycles of rigid-body refinement the R factor, R_{free} and FOM converged to 0.298, 0.301 and 0.754, respectively. This was followed by ten cycles of restrained isotropic temperature-factor refinement, after which the three statistics had converged to 0.273, 0.290 and 0.764, respectively. Maps were generated and visualized; residue-by-residue inspection of the protein followed and showed that the model fitted the electron-density maps. At this stage, 309 waters were found and four residue side chains were refitted, but only 268 waters were accepted. The structure underwent three more iterations of refinement (each consisting of ten cycles); each involved inspecting the protein density, adding new waters and deleting waters that failed to meet the criteria. The three statistical values converged to 0.214, 0.238 and 0.812, respectively, with 416 waters in the model. 34 residues showed some noticable excess $F_o - F_c$ density or partial excess $2F_o - F_c$ density features. After refitting the densities of five further side chains and accepting 51 new waters, the model was refined to the final statistics R factor = 0.211, R_{free} = 0.237 and FOM = 0.813. At this stage, it was found that both residues 181*A* and 181*B* were really Leu and not Val as in the starting model and the two residues were accordingly remodelled as Leu181*A* and Leu181*B* (see Figs. 4 and 5). At this stage, 1998 reflections were also removed from the 2.239–2.279 and 1.912–1.937 Å shells because of ice rings. After one iteration of restrained isotropic refinement and another iteration of restrained anisotropic refinement, the statistics converged to R factor = 0.190, R_{free} = 0.216 and FOM = 0.844. Maps were generated at this stage and Leu181*A* was again refitted; seven residues were also found with multiple conformations and implemented in the final iteration of the refinement. In this last iteration of restrained anisotropic refinement the statistics converged to R factor = 0.189, R_{free} = 0.215 and FOM = 0.846 (see Table 3). The final model contained two MPDs, two sulfate ions and 467 water molecules.

6. *B* factor per residue plots

The *B* factors (averaged for each atom of the side chain) were plotted against residue numbers for the three cases: apocrustacyanin C_1 (Gordon *et al.*, 2001), apocrustacyanin A_1 (Cianci *et al.*, 2001) and apocrustacyanin C_2 (this study, 1.3 Å model). The plots[1] showed where the three cases might differ. On checking the maps of the residues concerned, however, it was difficult to be convinced of a possible side-chain modification arising from disorder or a mobility effect on the electron density. These plots were extended by producing plots[1] of ΔB factors from the three pairs of data sets *versus* residue

[1] Supplementary data have been deposited in the IUCr electronic archive (Reference: FW5008). Details of services for acccessing these data are described at the back of the journal.

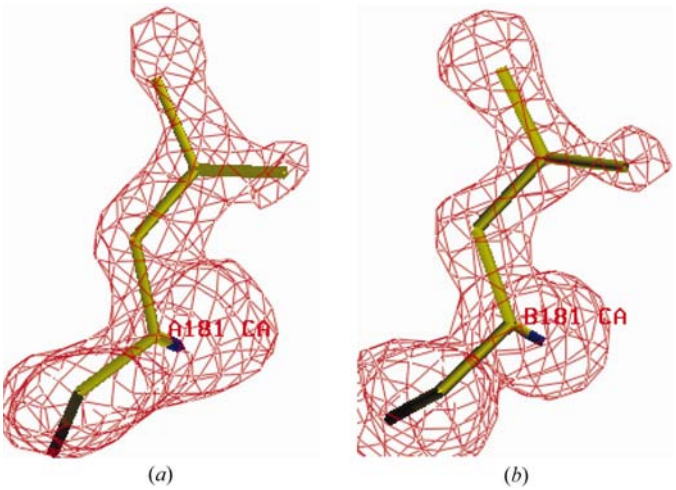

Figure 5
Section of omit protein electron-density map at 2.5 r.m.s. contour level for apocrustacyanin C_2 to 1.3 Å resolution. (*a*) Leu181*A*, (*b*) Leu181*B*.

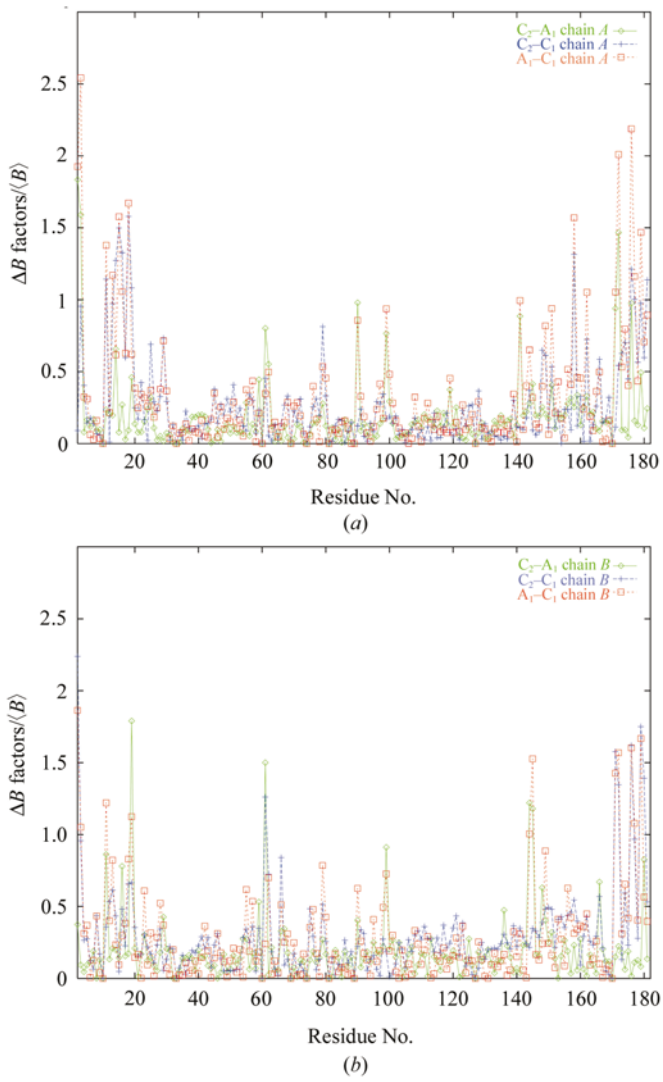

Figure 6
ΔB factors/$\langle B\rangle$ *versus* residue numbers for the structures of apocrustacyanin C_2, apocrustacyanin C_1 and apocrustacyanin A_1; C_2–A_1 in green, C_2–C_1 in blue and A_1–C_1 in red. (*a*) Chain *A*, (*b*) chain *B*.

numbers and further plots of (ΔB factors/$\langle B\rangle$) *versus* residue numbers (Fig. 6). These plots led to new residues being checked *via* omit maps. Careful examination of the $2F_o - F_c$ electron-density maps showed however that post-translational modifications involving N to O as in Asp–Asn and Glu–Gln or *vice versa* cannot be determined reliably solely by crystallography.

7. Discussion and conclusions

The diffraction quality of the apocrustacyanin C_2 crystal data has been improved from 2.2 Å (Wright *et al.*, 1992) to 1.3 Å and high-quality structure models developed based on molecular replacement to 1.6 Å (with glycerol) and to 1.3 Å (without glycerol). The latter improvement, 1.6 to 1.3 Å, we believe to arise from the use of longer exposure times. Glycerol was found to bind at the astaxanthin site and also at the MPD site. Cianci *et al.* (2001) suggested two post-translational modifications in apocrustacyanin A_1 compared with the model of the apocrustacyanin C_1 structure. One included an Asp to Asn modification of residue 5 and the other a total side-chain modification of Leu to Val of the C-terminal residue 181. The refinement of apocrustacyanin C_2 and the maps produced confirm that the modifications of residues 181*A* and 181*B* in apocrustacyanin A_1 were not valid for apocrustacyanin C_2 (Figs. 2 and 3). Residues 181*A* and 181*B* remodelled for apocrustacyanin A_1 fitted well as Leu, proving there is no mutation at residue 181 in apocrustacyanin A_1. Residues 5*A* and 5*B* were kept as Asn in C_2 as in the starting model of the A_1 structure. Visual inspection of the polypeptide side-chain density omit maps did not reveal any difference in amino-acid sequence between the homologous CRTC apoproteins. This is consistent with the isolation of a single gene for these proteins (Findlay, personal communication). Nevertheless, these proteins are separate entities in PAGE,[2] with the order of increasing negativity being C_2, C_1 and A_1. Superimposition of the crystal structures of the three apoproteins failed to reveal any significant difference in folding to explain this heterogeneity. To explain this PAGE signature (Fig. 1) post-translational modification may be envisaged involving Asn and/or Gln hydrolysis to acids, but occurring at susceptible (exposed) residues in the macromolecular α-crustacyanin. These modifications need not be identical in each subunit, but would depend on the configurational arrangement of the subunits in the complex. Facile deamidation of protein Asn and Gln residues occurs during storage of proteins in ammonium sulfate solution and at high ionic strength (Scotchler & Robinson, 1974; McKerrow & Robinson, 1971), the means used for extracting and storage of α-crustacyanin. Unselective amide hydrolysis, however, would lead to an infinite number of entities. It is noted that Asn at

[2] The PAGE gel (Fig. 1) is run at pH 8.5 at which pH the apoproteins are negatively charged. The bottom of the gel is positive *i.e.* this is the charge of the electrode at the bottom of the gel to which the proteins are running and the top is negative *i.e.* the charge of the electrode at the top end of the gel. So, the most negative protein runs fastest to the bottom of the gel *i.e.* A_1 is most negative, then C_1 less negative, then C2 is the least negative.

residue 5 in apocrustacyanin (Cianci *et al.*, 2001) as the sole change would make this protein less negative than apocrustacyanin C_1, the reverse of what is observed. However, the difference in the X-ray scattering factors of nitrogen and oxygen is small and not clearly visible at the present resolutions. Overall, it is indeed a difficult task to distinguish between Asn/Asp or Gln/Glu in these X-ray crystal structures. Factors such as disorder or mobility also might distort the electron density of a particular atom or residue. The efforts described here of *B* factor per residue plots and their normalized differences, substantiate the sequence identity for the three homologous CRTC apoproteins as expressed by a single gene, but failed to identify any post-translational modifications. It is likely that the differences lie in Asn/Asp and/or Gln/Glu changes, the result of selective deamination on storage of crustacyanin or of selective deamination by specific post-translational modification. A detailed mass-spectroscopy study (see, for example, Wilkins *et al.*, 1999) is required to identify any amide/acid differences and the sites of alteration.

The salaries of JH and GAN were supported by The Leverhulme Trust under a research grant awarded to JRH, NC and PFZ. Analysis of the structures was undertaken in the University of Manchester Laboratory of Structural Chemistry using the SG workstation suite funded originally by the BBSRC and The Wellcome Trust, to whom JRH is also very grateful. Synchrotron-radiation beamline MPW14 was used for data collection and we are therefore very grateful to Daresbury Laboratory SRS for this provision *via* a BBSRC block allocation of beam time award.

References

Chayen, N. E., Cianci, M., Grossmann, J. G., Habash, J., Helliwell, J. R., Nneji, G. A., Raftery, J., Rizkallah, P. J. & Zagalsky, P. F. (2003). *Acta Cryst.* D**59**, 2072–2082.

Chayen, N. E., Gordon, E. J. & Zagalsky, P. F. (1996). *Acta Cryst.* D**52**, 156–159.

Cianci, M., Rizkallah, P. J., Olczak, A., Raftery, J., Chayen, N. E., Zagalsky, P. F. & Helliwell, J. R. (2001). *Acta Cryst.* D**57**, 1219–1229.

Cianci, M., Rizkallah, P. J., Olczak, A., Raftery, J., Chayen, N. E., Zagalsky, P. F. & Helliwell, J. R. (2002). *Proc. Natl Acad. Sci. USA*, **99**, 9795–9800.

Collaborative Computational Project, Number 4 (1994). *Acta Cryst.* D**50**, 760–763.

Duke, E. M. H., Kehoe, R. C., Rizkallah, P. J., Clarke, J. A. & Nave, C. (1998). *J. Synchrotron Rad.* **5**, 497–499.

Findlay, J. B. C., Pappin, D. J. C., Brett, M. & Zagalsky, P. F. (1990). In *Carotenoids: Proceedings of the 8th International Symposium on the Carotenoids, Boston, July 1987*, edited by N. I. Krinsky, M. M. Mathews-Roth & R. F. Taylor. New York: Plenum Press.

Gordon, E. J., Leonard, G. A., McSweeney, S. & Zagalsky, P. F. (2001). *Acta Cryst.* D**57**, 1230–1237.

Habash, J., Boggon, T. J., Raftery, J., Chayen, N. E., Zagalsky, P. F. & Helliwell, J. R. (2003). *Acta Cryst.* D**59**, 1117–1123.

Jones, T. A., Zou, J. Y., Cowan, S. W. & Kjeldgaard, M. (1991). *Acta Cryst.* A**47**, 110–119.

Keen, J. N., Caceres, I., Eliopoulos, E. E., Zagalsky, P. F. & Findlay, J. B. C. (1991). *Eur. J. Biochem.* **197**, 407–417.

Leslie, A. G. W. (1992). *Jnt CCP4/ESF–EACMB Newsl. Protein Crystallogr.* **26**, 27–33.

McKerrow, J. H. & Robinson, A. B. (1971). *Anal. Biochem.* **42**, 565–568.

Olczak, A., Cianci, M., Hao, Q., Rizkallah, P. J., Raftery, J. & Helliwell, J. R. (2003). *Acta Cryst.* A**59**, 327–334.

Quarmby, R., Norden, D. A., Zagalsky, P. F., Ceccaldi, H. J. & Dumas, R. (1977). *Comp. Biochem. Physiol. B*, **56**, 55–61.

Scotchler, J. W. & Robinson, A. B. (1974). *Anal. Biochem.* **59**, 319–322.

Wilkins, M. R., Gasteiger, E., Gooley, A. A., Herbert, B. R., Molloy, M. P., Binz, P.-A., Ou, K., Sanchez, J.-C., Bairoch, A., Williams, K. L. & Hochstrasser, D. F. (1999). *J. Mol. Biol.* **289**, 645–657.

Wright, C. E., Rafferty, J. B., Flower, D. R., Groom, C. R., Findlay, J. B. C., North, A. C. T., Phillips, S. E. V. & Zagalsky, P. F. (1992). *J. Mol. Biol.* **224**, 283–284.

Zagalsky, P. F. (2003). *Acta Cryst.* D**59**, 1529–1531.

Zagalsky, P. F. & Tidmarsh, M.-L. (1985). *Comp. Biochem. Physiol. B*, **80**, 599–601.